

A Solar Prominence Model

Jan Kuijpers

Sterrekundig Instituut, Universiteit Utrecht, Postbus 80 000, 3508 TA Utrecht
Dep. of Exp. High Energy Physics, University of Nijmegen, 6525 ED Nijmegen
CHEAF, 1009 DB Amsterdam, The Netherlands

Received _____; accepted _____

Submitted to ApJ Letters

ABSTRACT

We propose a model for solar prominences based on converging flow observed in the chromosphere and photosphere. In contrast with existing models we do not apply a shearing motion along the neutral line. Instead we assume that bipolar loops approaching on different sides of the neutral line have a non-vanishing magnetic helicity of the *same* sign. In the converging flow the individual loops kink and develop a skew. For loops of the same helicity the skew is in the same sense. As a result the ‘chiral’ symmetry of an aligned distribution of loops is broken and the reconnecting loop system forms a filament with the observed magnetic orientation and anchoring of the barbs in regions of parasitic polarity. The filament consists of a number of individual strands of coaxial coronal electric currents each of which is current neutralised. The filament material is suspended in dips in the magnetic field and the transverse field direction coincides with that in the Kuperus-Raadu model. Above the filament a cavity forms with an overlying arcade consisting of the outer portions of the reconnected loops.

Subject headings: Sun: magnetic fields — Sun: filaments — Sun: prominences — Sun: corona — MHD

1. Introduction

Solar prominences or filaments occur above boundaries of *converging* photospheric flows (Martin 1986, Rompolt & Bogdan 1986), located between opposite polarity magnetic fields (Martin 1990). Along these ‘polarity inversions’ magnetic flux disappears (flux cancelling).

The intermediate legs or appendages along the sides of a quiescent filament are rooted in magnetic fields opposite in polarity to the network magnetic fields on the same side (Martin et al. 1994, Martin & Echols 1994). Not only is the perpendicular component of the field reversed but also the axial component is opposite to what would be expected from differential rotation acting on coronal arcades (Leroy et al. 1983). This ‘inverse’ configuration has been called the ‘Double Inverse Polarity Paradigm’ (Kuperus 1996).

Quiescent filaments are predominantly *dextral* – i.e. the field direction in the filament is to the right for an imaginary observer in the chromosphere on the positive-polarity side and facing the broad side of the filament – in the *northern* solar hemisphere, and *sinistral* in the southern hemisphere, independent of the solar cycle (Martin et al. 1994).

Below I will take these observations – the *converging migration of fields*, and the association of the ends of a filament with network magnetic fields of *opposite polarity* – as the starting point for an evolutionary model of a quiescent filament. I will show that a successful filament model obtains if one starts off with bipolar loops with the *same magnetic helicity* on both sides of the polarity inversion line. No assumption on the existence of a shearing flow will be needed. The current structure of the proposed filament model consists of an aligned row of ‘neutralised’ currents, each with coaxial current closure. The mass and the mass motions inside the filament result from intermittent internal and external reconnections, subsequent impulsive heating, chromospheric evaporation, cooling and

condensation inside individual twisted flux tubes.

2. Filament formation from reconnecting twisted loops

2.1. A single flux tube in converging flow

Consider a single twisted flux tube, rooted below the photosphere. In the ideal MHD approximation the free magnetic energy of the tube – stored in coronal electric currents – *increases* as the footpoints approach each other. This can be seen as follows: the free magnetic energy of a tube W_f is given by the azimuthal component of the magnetic field, which derives from the axial current. As the number of windings between the footpoints of an individual field line is fixed in ideal MHD while the tube length L decreases, the azimuthal field component varies approximately as $B_\phi = B_z R/L$, and increases as L decreases (B_z is the axial magnetic field component and R the ‘minor radius’ of the tube). As the (axial) magnetic flux is conserved we then have for the free magnetic energy

$$W_f = \int \frac{B_\phi^2}{2\mu_0} d^3\vec{r} \propto L^{-1}. \quad (1)$$

Let us apply the Poynting theorem to a loop anchored in converging motion at the photospheric boundary. It then follows (from the term with $\vec{v} \cdot \vec{B} \vec{B} \cdot d\vec{S}$, velocity \vec{v} , magnetic field \vec{B} , surface element $d\vec{S}$) that during a temporal increase in total magnetic energy the legs of the loop diverge away from each other into the corona.

A *force free* structure can only store a certain amount of energy which is dictated by the magnetic field distribution at its bounding surface, as follows from the scalar magnetic virial theorem (Aly 1985, Low 1986). Asymptotically, an increase in magnetic energy corresponds to a decreasing tangential component and an opening up of the field lines. As a result a

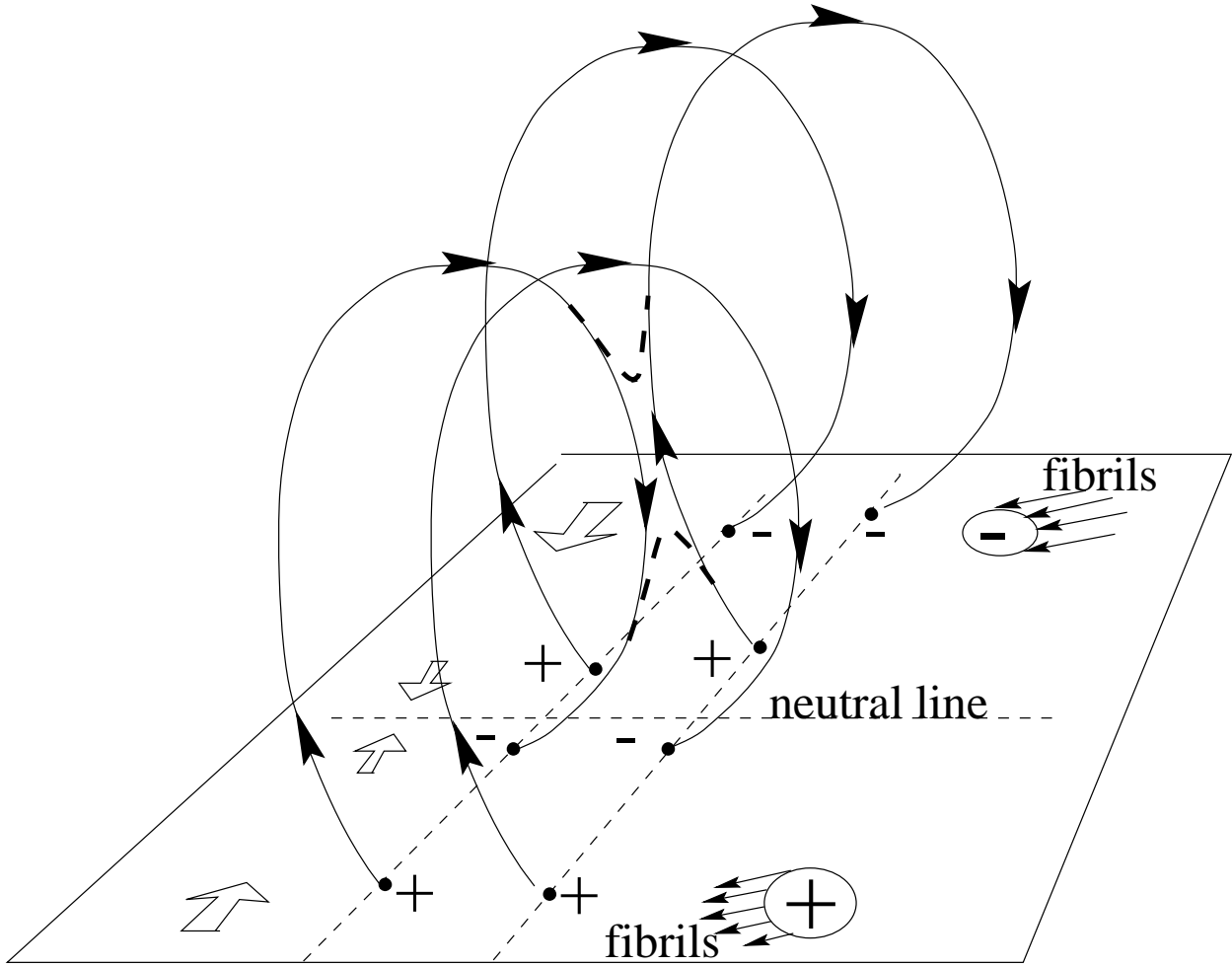


Fig. 1.— Perspective view of four bipolar loops with the same sense of helicity and migrating towards the neutral line separating domains of dominant positive (+) and negative (-) polarity (marked by a small circle from (into) which H- α fibrils start (end)). Reconnection is indicated with heavy dashed lines.

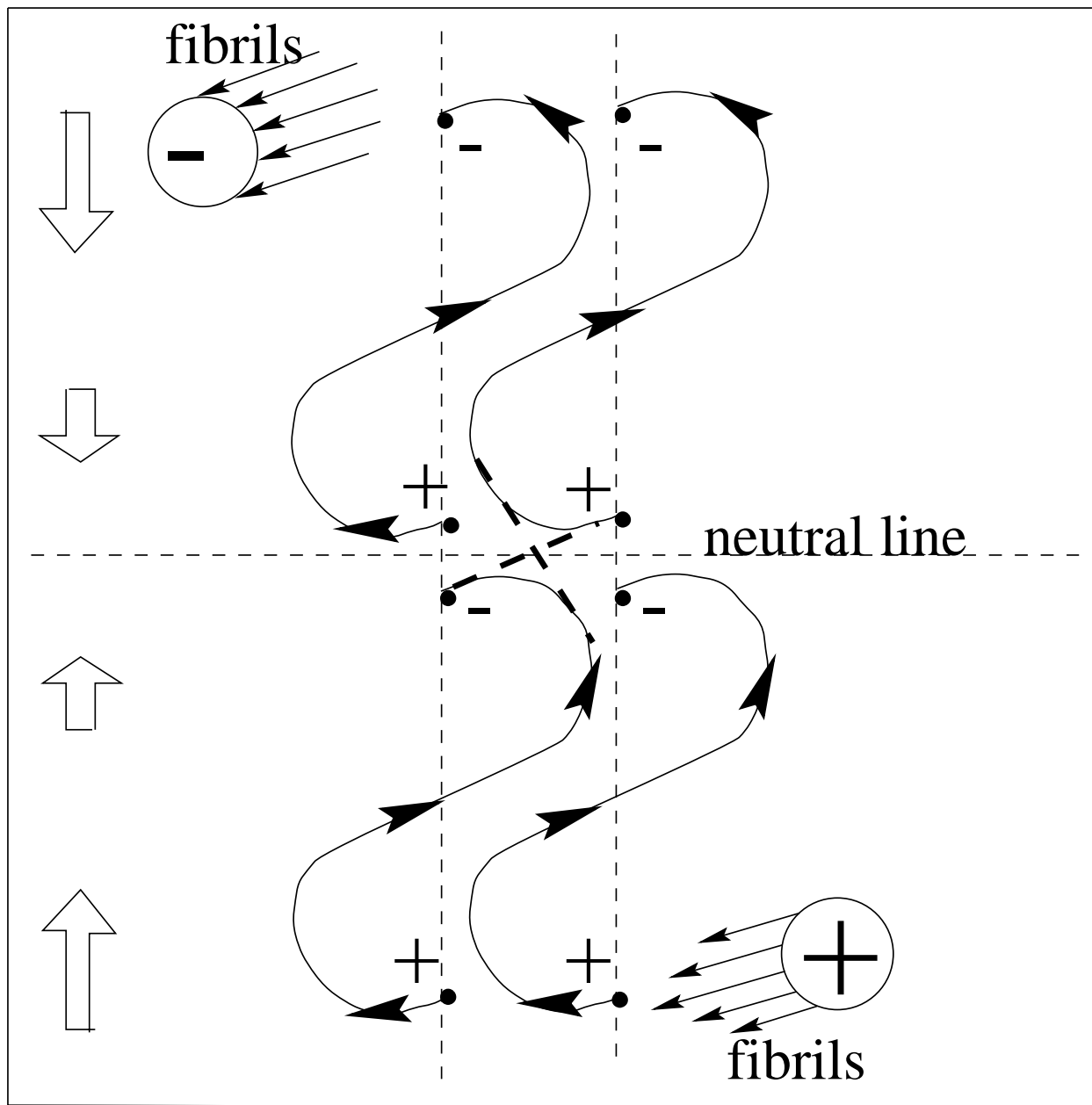


Fig. 2.— Top view of Fig. 1. Heavy dashed curves indicate reconnection.

force free coronal flux tube expands *upward* at the same time when the footpoints converge and the free energy, defined as the energy stored in coronal electric currents, increases.

Further, as the azimuthal field component in the tube increases with respect to the axial component the 3-D tube kinks (Finn et al. 1994) and buckles sideways in the same sense as the original twist, thereby introducing a systematic *skew*. The above three effects – the diverging legs of an individual loop, its expansion upward, and its buckling – are sketched in Figs. 1 and 2 where four loops are anchored in a converging flow pattern such that the internal separation of each pair of footpoints of the four loops decreases in time.

Actually, the twist and buckling are quantitatively best described by the concept of magnetic *helicity* of a magnetically closed volume (Berger & Field 1984, Berger 1984, Berger 1988, Moffat 1969). A flux tube can only be observed as far as it extends above the photosphere and, strictly speaking, this part is not bounded by a magnetic surface. It has been shown (Berger & Field 1984) that in this case one can define a relative helicity which essentially is the coronal part. In ideal MHD the helicity of any flux tube is conserved under its motion (Woltjer 1958) and this underlies the twisted shape of the flux tubes in Figs. 1 and 2, where, to be definite, we have assumed a direction of the current on the magnetic axis of each tube *parallel* to the magnetic field (and a return current on the surface of the tube).

2.2. Multiple flux tubes in converging flow

We now drop the ideal MHD assumption and allow for magnetic reconnection to take place. In this case one can still define the total magnetic helicity of the system of reconnecting flux tubes, which, according to Taylor’s conjecture is a conserved quantity (Taylor 1974, Taylor 1986). In Figs. 1 and 2 a number of flux tubes with parallel orientation

and the same sign of magnetic helicity are anchored in a converging flow pattern on both sides of the line of convergence – the magnetic neutral line between two largely unipolar regions. As the helicity in a force free flux tube causes a symmetry breaking of the shape of each tube as sketched in Figs. 1 and 2, reconnection between tubes on different sides of the neutral line leads to a system of inner and outer arches. Figs. 3 and 4 picture the relaxed state after reconnection between two of the loops in Figs. 1 and 2 has occurred. Note that the inner tube is highly sheared although no shearing motion has been applied. Thus reconnection leads to a sheared inner row of ‘neutralised’, coaxial current loops. Moreover, the inner strands have a magnetic field orientation as is observed in quiescent filaments, that is they are anchored in parasitic polarities. Note that eventually the flux of these parasitic polarities is cancelled as they submerge in the converging flow pattern, and the dominant polarities on both sides of the neutral line are ‘cleaned’. In this picture the elements of a filament are episodically destroyed and replaced. Also, further reconnection between the inner strands can lead to a few extended loops in the axial direction, bridging the region of downflow and escaping destruction. Finally, the outer row of reconnected loops have a twist which agrees with the observed streaming direction of fibrils bordering a filament channel.

On average the radiative loss in a prominence should balance the heating, which we assume to derive from magnetic reconnection of the loops in the converging flow pattern. Putting the average heating rate per unit volume equal to the Poynting flux one obtains

$$E_H \approx \frac{vB^2}{2\mu_0 D} = 3.58 \cdot 10^{-4} \text{ W m}^{-3} \quad (2)$$

for a global convergence speed $v \approx 0.1$ km/s, a typical prominence field of 0.003 T and a horizontal width transverse to the neutral line of $D \approx 1$ Mm. Indeed this rate is of the same order as radiative cooling in the central part of the prominence, which for an electron density $n_e = 10^{17} \text{ m}^{-3}$ and a temperature of 8000 K (the Hvar reference model, Tandberg-Hanssen 1995) amounts to $E_{rad} \approx 3 \cdot 10^{-4} \text{ W m}^{-3}$.

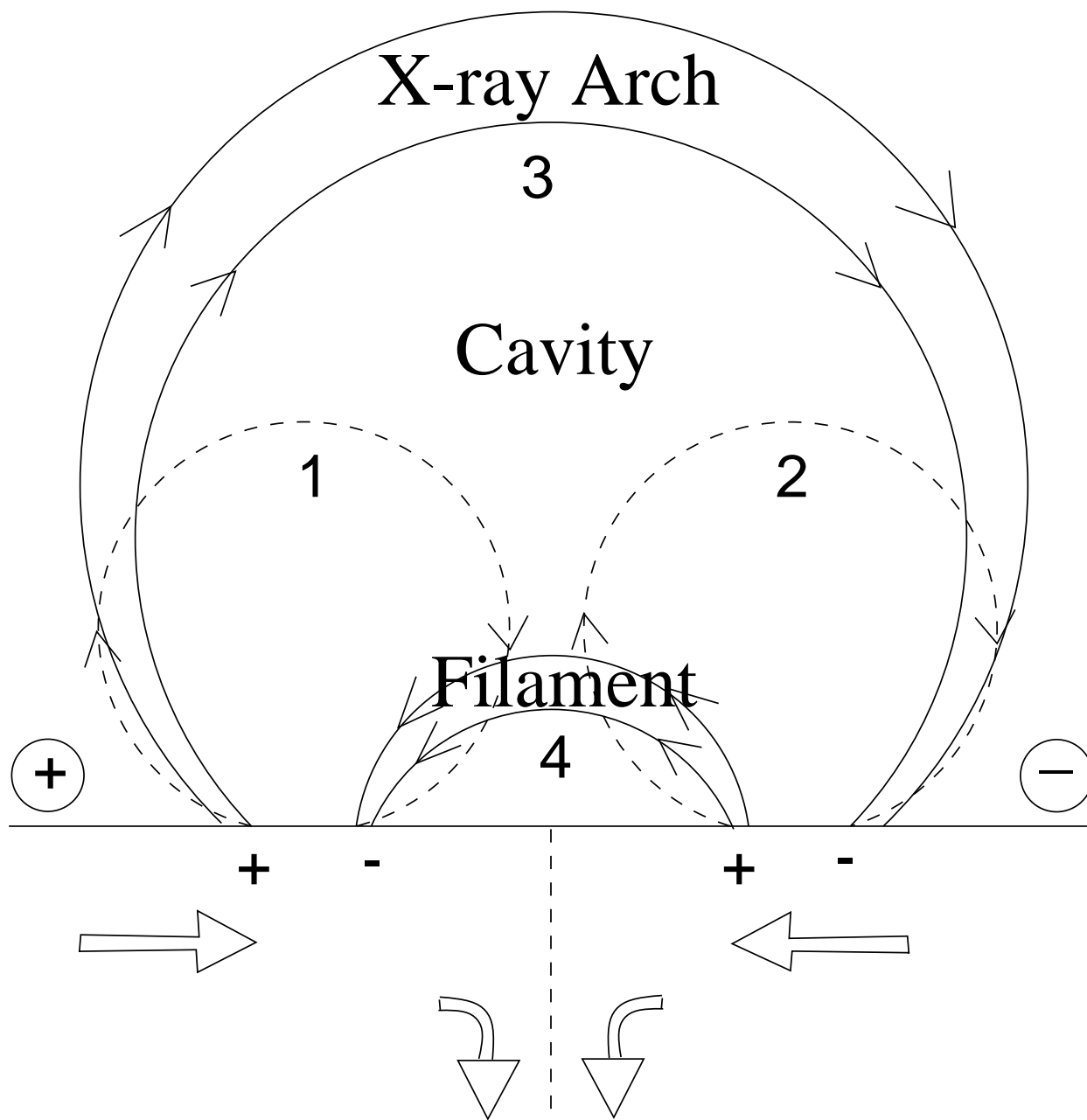


Fig. 3.— Side view of Figs. 1 and 2 in the direction of the neutral line, before (dashed) and after (drawn) reconnection.

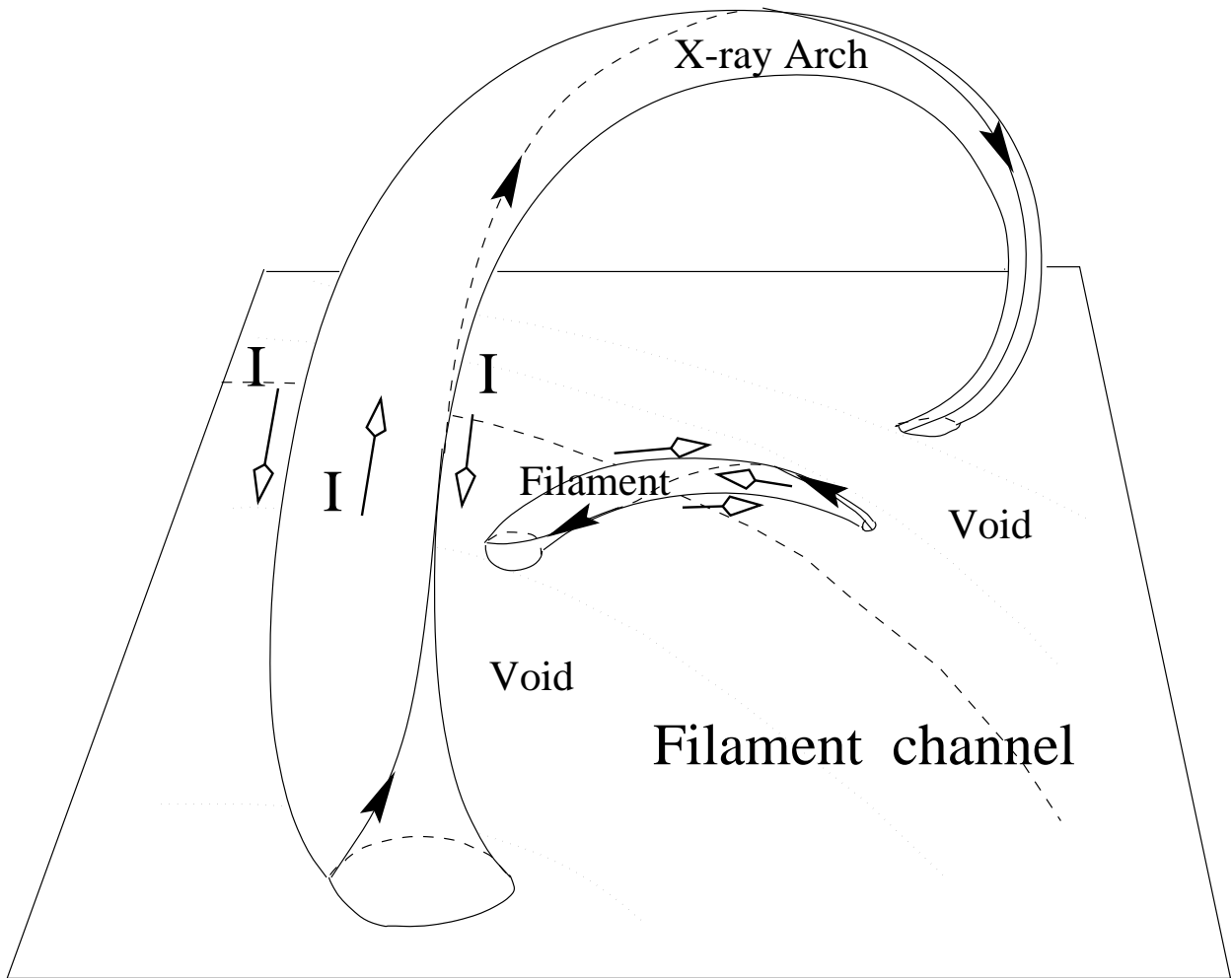


Fig. 4.— Perspective view of a single elementary loop in the filament and in the overlying arcade. The directions of the electric currents I are indicated with open arrows.

Now, energy release by reconnection occurs in bursts with a typical time scale of a few Alfvén crossing times of the reconnecting structure. Let us assume that reconnection events occur randomly inside thin flux tubes crossing the neutral line at a rate of about 10^{-3} Hz and that each takes 1 s (corresponding to a reconnection over 100 km and an average converging flow of 0.1 km/s). Then the instantaneous heating rate in the flux tube goes up by a factor 10^3 and reaches a value 0.3 W m^{-3} . At this rate and for a gas pressure $p = 0.02 \text{ N m}^{-2}$, the quantity E_H/p^2 is nearly an order of magnitude larger than the maximum in the quantity $\Psi(T)/(2k_B T)^2$ at which steady state coronal loops can exist (van den Oord & Zuccarello 1997, $\Psi(T)$ is the radiative loss function). Clearly, such a heating is so impulsive that it must lead to strong evaporation of chromospheric material into the loop and subsequent radiative cooling below 10^4 K (cf. also Poland & Mariska 1986). The condensed gas becomes visible as part of the filament, and can be sustained against gravity in a dip of the twisted flux tube (Amari et al. 1991, Démoulin & Priest 1993), at least temporarily as long as the tube remains above the chromosphere.

3. Coronal cavity and arcade

Heating by reconnection in the outer loops would lead to an X-ray arcade. From the geometry of the reconnecting loops (Fig. 3) it follows that the sites of lower and upper reconnection are separated by a quiescent volume or cavity. Reconnection in the overlying arcade again causes heating at an average rate given by Eq. (2). However as both the field strength is lower and the dimensions are larger (typically $B = 10^{-4}$ T and $D = 30$ Mm) the heating rate per unit volume is at least four orders of magnitude smaller, $E_H \approx 1.3 \cdot 10^{-8} \text{ W m}^{-3}$. For such values steady hot coronal loops can exist without a problem (van den Oord & Zuccarello 1997). Multiple reconnection events then again lead to evaporation but now a hot coronal arcade is maintained as the footpoints converge.

Both the filament and the arcade can go unstable because both are essentially force free equilibrium structures which tend to expand as the total current increases. The first would show up as a filament flare, the latter as a Coronal Mass Ejection (CME). Note that the proposed mechanism would explain why a CME has already an enhanced density before the explosion occurs. Also the finite gas pressure may have an important effect on the CME instability (Zwiggmann 1987).

The only practical complication in describing the filament flare is the large number of neutralised currents, which can not be modelled by a simple circuit. The occurrence of instability is determined by the magnitude of the current system which depends on the number of reconnected bipolar loops, their initial currents, and the footpoint displacement. Interestingly, in our model each of these quantities would be correlated in the arcade and in the prominence. This effect may dissolve the long-standing debate about the relation between CMEs and flares. In the present model both are indeed ‘signatures of the same disease’ (Harrison 1995). Here it is of interest to mention the numerical simulation of a converging, quadrupolar, arcade (however, without submerging central flow) presented by Dr. Uchida at the recent IAU Symp. No. 188 in Kyoto (Uchida 1997).

4. Discussion

Quiescent prominences in the same hemisphere are observed to have the same handedness independent of solar cycle. Here we have shown how a converging flow in an ordered series of bipoles with the same sense of helicity would lead to the formation of prominences with the observed inverse polarity and the same handedness (dextral/sinistral). Magnetic loops rising upward inside the sun experience a Coriolis force and develop the same sense of helical distortion in the same hemisphere. If these distortions lead to a magnetic helicity the sense of the magnetic helicity would be independent of the loop

orientation and, consequently, independent of the solar cycle.

Both the quasi-steady high density at coronal temperatures in an arcade and the non-steady high density at a low temperature in a filament are caused by reconnections, the difference in appearance being the result of a dramatic difference in volume heating rates caused by a difference in dimensions. The observed upward flows (5 km/s in CIV and 0.5 km/s in H- α , Schmieder 1989) are entirely consistent with cooling gas flows after evaporation from impulsive reconnection events. Also the excellent fit of a prominence shape by a linear force free field (Schmieder et al. 1989) is consistent with magnetic relaxation satisfying Taylor’s conjecture. Finally, in our model the horizontal component of an extended non-potential field – which is held to cause alignment of fibrils at the border of a filament channel (Gaizauskas et al. 1997) – derives from electric currents in the outer reconnected loops while reconnections of sheared inner loops lead to the appearance of a filament.

The present model starts off from a collection of dipoles without any net magnetic flux in the direction of the neutral line. As soon as chiral symmetry is lost such an ‘axial’ component is created in the corona (see Figs. 1 and 2), and persists after reconnection. However, the *net* axial flux, summed over the arch and the filament, remains zero. This seems to be in conflict with observations at lower latitudes (Martin & McAllister 1996) but in agreement with polar crown arcades (McAllister et al. 1997).

How does our proposal relate to existing models? Ours is essentially dynamical and depends on ongoing reconnection between bipolar loops of the same helicity in a converging flow pattern. It therefore differs from the model by van Ballegooijen & Martens (1989) which requires a shearing motion. The quasistatic support of gas against gravity in our model is in dips as in the Kippenhahn-Schlüter (KS) model (Kippenhahn & Schlüter 1957). A difference with the latter is that the existence of (largely force free) currents is essential

to the present mechanism while force free currents are absent in the KS case. Therefore the dips can be primarily of a force free nature. This practically force free aspect is an essential ingredient also of the Kuperus-Raadu (KR) model (Kuperus & Raadu 1974). A difference with the latter model is that the currents in the present model are largely coronal with coaxial return currents, while in the KR model the coronal current has a unique direction and the return current is in the photosphere/chromosphere.

I would like to thank Sara Martin, Bert van den Oord, Max Kuperus, and the referee for their comments.

REFERENCES

- Aly, J.J. 1985, *A&A*, 143, 19
- Amari, T., Démoulin, P., Browning, P., Hood, A.W., Priest, E.R. 1991, *A&A*, 241, 604
- Berger, M.A. 1984, *Geophys. Astrophys. Fluid Dynamics*, 30, 79
- Berger, M.A. 1988, *A&A*, 201, 355
- Berger, M.A., & Field, G.B. 1984, *J. Fluid Mech.*, 147, 133
- Démoulin, P., & Priest, E.R. 1993, *Solar Phys.*, 144, 283
- Finn, J.M., Guzdar, P.N., Usikov, D. 1994, *ApJ*, 427, 475
- Gaizauskas, V., Zirker, J.B., Sweetland, C., Kovacs, A. 1997, *ApJ*, 479, 448
- Harrison, R.A. 1995, *A&A*, 304, 585
- Kippenhahn, R., & Schlüter, A. 1957, *Z. Astrophys.*, 15, 36
- Kuperus, M. 1996, *Sol. Phys.*, 169, 349
- Kuperus, M., & Raadu, M.A. 1974, *A&A*, 31, 189
- Leroy, J.L., Bommier, V., Sahal-Bréchet, S. 1983, *Sol. Phys.*, 83, 135
- Low, B.C. 1986, *ApJ*, 307, 205
- Martin, S.F. 1986, in *Coronal and Prominence Plasmas*, ed. A.I. Poland, NASA Conf. Publ. 2442 (Greenbelt: GSFC), 73
- Martin, S.F. 1990, in *Dynamics of Quiescent Prominences*, IAU Coll. No. 117, ed. V. Ruždjak & E. Tandberg-Hanssen (Berlin: Springer Verlag), 1

- Martin, S.F., & Echols, C.R. 1994, in *Solar Surface Magnetism*, ed. R.J. Rutten & C.J. Schrijver (Dordrecht: Kluwer Acad. Publ.), 339
- Martin, S.F., & McAllister, A.H. 1996, *BAAS* 27, 961
- Martin, S.F., Bilimoria, R., Tracadas, P.W. 1994, in *Solar Surface Magnetism*, ed. R.J. Rutten & C.J. Schrijver (Dordrecht: Kluwer Acad. Publ.), 303
- McAllister, A.H., MacKay, D., Hundhausen, A.J., Priest, E. 1997, *BAAS*, 29, 903
- Moffat, H.K. 1969, *J.Fluid. Mech.*, 35, 117
- Poland, A.I., & Mariska, J.T. 1986, *Solar Phys.*, 104, 303
- Rompolt, B., & Bogdan, T. 1986, in *Coronal and Prominence Plasmas*, ed. A.I. Poland, NASA Conf. Publ. 2442 (Greenbelt: GSFC), 81
- Schmieder, B. 1989, in *Dynamics and Structure of Quiescent Solar Prominences*, ed. E.R. Priest (Dordrecht: Kluwer Acad. Publ.), 15
- Schmieder, B., Raadu, M.A., Démoulin, P., Dere, K.P. 1989, *A&A*, 213, 402
- Tandberg-Hanssen, E. 1995, *The Nature of Solar Prominences* (Dordrecht: Kluwer Acad. Publ.), Table 3.4, Fig. 4.6
- Taylor, J.B. 1974, *Phys. Rev. Lett.*, 33, 1139
- Taylor, J.B. 1986, *Rev. Modern Phys.*, 58, 741
- Uchida, Y. 1997, in *The Hot Universe*, IAU Symp. No. 188, ed. S. Kitamoto (Dordrecht: Kluwer Acad. Publ.), to appear
- van Ballegooijen, A.A., & Martens, P.C.H. 1989, *ApJ*, 343, 971
- van den Oord, G.H.J., & Zuccarello, F. 1997, *A&A*, submitted, Fig. 2a

Woltjer, L. 1958, Proc. Nat. Acad. Sci., 44, 489

Zwingmann, W. 1987, Solar Phys., 111, 309